

**Design, Fabrication, Testing of an Optical Sensor to Measure Effective Retinal Cone
Illuminance In Situ**

BY

GIACOMO D'ALESSANDRO

MSc, Politecnico di Milano, Milan, Italy, 2017

MSc, Politecnico di Torino, Turin, Italy, 2017

BSc, Politecnico di Milano, Milan, Italy, 2015

THESIS

Submitted as partial fulfillment of the requirements
for the degree of Master of Science in Bioengineering
in the Graduate College of the
University of Illinois at Chicago, 2018

Chicago, Illinois

Defense Committee:

John R. Helting, Chair and Advisor

Anthony E. Felder

Riccardo Barbieri, Politecnico di Milano

ACKNOWLEDGEMENTS

First and foremost, I would like to express my sincere gratitude to Prof. John R. Hetling for giving me the possibility to participate to this thesis and to work in his laboratory at UIC, making my experience in Chicago memorable from a professional and personal point of view.

I also want to thank all my colleagues that joined me in this joint master between Politecnico di Milano and UIC and for all the experiences that we shared in this period.

I also want to personally thank Verdiana Carini who is a friend, colleague and travel mate, for her precious help and support day by day.

Finally, a special sense of gratitude for my parents that have supported me during my whole academic career, in all the moments and experiences that I have done.

TABLE OF CONTENTS

CHAPTER	PAGE
1. INTRODUCTION	1
1.1 Gross anatomy and optical structure of the eye	1
1.2 Problem statement.....	5
1.3 Previous measurements of relative retinal illuminance	5
1.4 Light measurement terminology	6
2. SPECIFIC AIM 1: FABRICATE AN OPTICAL SENSOR SYSTEM THAT MEASURES LOCAL EFFECTIVE ILLUMINANCE IN ABSOLUTE UNITS	8
2.1 Specific Aim 1 Methods	8
2.1.1 Construction of Cone-view Sensor	8
2.1.2 Stimulus Source	10
2.2 Specific Aim 1 Results.....	11
2.2.1 Calibration of the cone-view sensor	12
3. SPECIFIC AIM 2: MEASURE THE RETINAL ILLUMINANCE IN SHEEP EYES	13
3.1 Specific Aim 2 Methods	13
3.1.1 Design of the eye holder and sensor positioning system	13
3.1.2 Measurement Protocol	15
3.1.3 Analysis Protocol	20
3.2 Specific Aim 2 Results.....	22
4. DISCUSSION	26
5. APPENDIX.....	28
6. REFERENCES	31

LIST OF FIGURES

FIGURES	PAGE
Figure 1: View of the human eye (webvision, 2012).....	1
Figure 2: Vertical sagittal section of the adult human eye (webvision, 2012).	2
Figure 3: Simple organization of the retina (webvision, 2012).	3
Figure 4: Representation of the Snell's Law.	4
Figure 5: UV/VIS light attenuation at specific wavelength (Edmund Scientific).	9
Figure 6: Cree XLamp MC-E LED (Cree Data Sheet).....	10
Figure 7: Scheme of the stimulus source positioning.	11
Figure 8: A schematic picture of the system realized with the main components: fiber core, fiber cladding, syringe; photopic filter and photosensor.	11
Figure 9: Cone view sensor. A. Frontal view of one end. It gets 2 mm outside the syringe. B. Up view.....	12
Figure 10: Eye holder and positioning system. Lateral view. 1. Lamp; 2. Eye holder ring; 3. Sensor holder; 4. Components for angular alignment.	13
Figure 11: Eye holder and positioning system. Frontal view. 1. Lamp; 2. Eye holder ring; 3. Sensor holder; 4. Components for angular alignment.	14
Figure 12: Eye holder and positioning system. Up view. 1. Lamp; 2. Eye holder ring; 3. Sensor holder; 4. Components for angular alignment.	14
Figure 13: Picture of the measurement system during an experiment. 1. Eye fixed with super glue; 2. Optic nerve; 3. Sensor inserted into the eye at 0°.	16
Figure 14: Up view of the measurement system during an experiment. 1. Eye fixed with super glue; 2. Optic nerve; 3. Sensor inserted into the eye at 0°.	17
Figure 15: Saline solution used to maintain pressure inside the eye.	18
Figure 16: Picture of an experiment in dark condition with the "cone-view" sensor at 45 degrees. 1. Eye; 2. Sensor at 45°; 3. Saline solution syringe.	19
Figure 17: Boxplot of the retinal illuminance before normalization for eye size at 0, 30 and 45 degrees.	23
Figure 18: Boxplot of the corrected illuminance values at different angles: 0, 30 and 45 degrees...	23
Figure 19: Comparison between our results and those reported by Koyjiman and Witmer (1986). Both data sets were normalized by dividing the mean and standard deviation at each angle by the mean observed at 0 degrees.	25

LIST OF TABLES

TABLE	PAGE
Table 1: DIMENSIONS OF THE 6 EYES TO CALCULATE THE CORRECTION FACTORS ..	20
Table 2: MEASUREMENTS OF RETINAL ILLUMINANCE IN ABSOLUTE VALUES [lm sr m^{-2}]	22

SUMMARY

This thesis has achieved the realization of the first sensor to measure effective retinal illuminance for cones in absolute units, approximating the acceptance angle of a cone photoreceptor cell, if positioned such that its axis is aligned in the anatomically correct orientation for cones at the locus of the measurement within the retina. The sensor designed is different from all the ones already found in literature because it approximates the optical properties of a cone photoreceptor cell. Till now, measurements obtained in literature have been referred only in relative values and we have provided a good measuring approach to obtain values in absolute units. A first test of the sensor has been done on sheep eyes that were the only ones available for the strict times and constraints of this work. The results have shown that retinal illuminance decreases more and more from the center of the retina (0 degrees) to different angles (30 – 45 degrees). The results have also shown that different eyes have similar measurements between them.

CHAPTER 1

INTRODUCTION

1.1 Gross anatomy and optical structure of the eye

The eye has a slightly asymmetrical spherical shape. Its dimensions are: sagittal diameter of about 24 mm, transverse one of 24 mm and volume of about 6.5 cc (Encyclopedia Britannica Macropedia, 1997). It has several structures, each with its own function (Fig. 1). The pupil allows the light to enter and it is composed by absorbing pigments that give it its dark color. The colored circular muscle, the iris, controls the size of the pupil and the light entering. The first lens is the cornea. The sclera, is the white part of the eye, and has a function of support (Kolb, 1991).

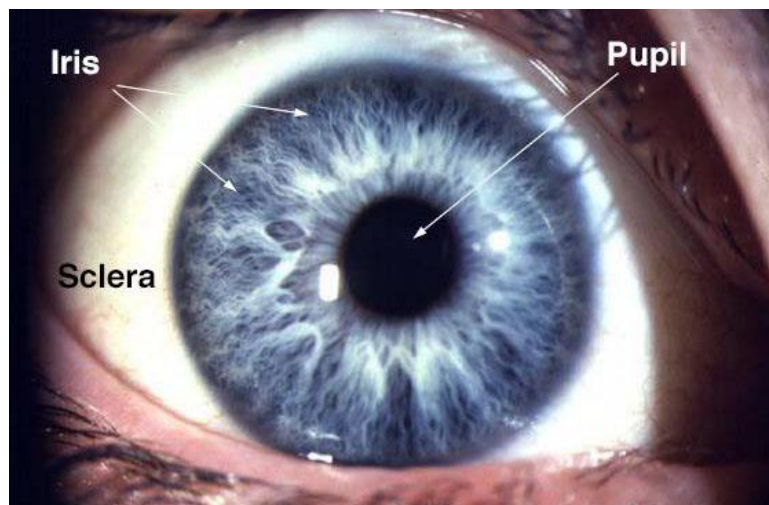


Figure 1: View of the human eye (webvision, 2012).

A cross-sectional view of the eye shows three different layers and three chambers of fluid (Fig. 2). It is constituted by three layers (external – sclera and cornea; intermediate – iris and ciliary body

and choroid; internal – retina) (Sally Wu). It also presents three chambers of fluid (anterior and posterior chambers filled with aqueous humor; vitreous chamber filled with vitreous humor).

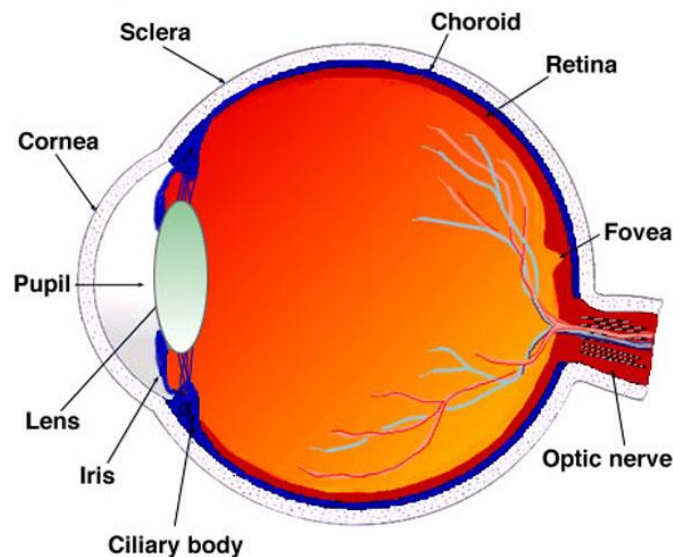


Figure 2: Vertical sagittal section of the adult human eye (webvision, 2012).

The retina is a hemispherical layer approximately 0.5 mm thick (Polyak, 1941; Van Buren, 1963; Kolb, 1991). The ganglion cells are the first cells encountered by light and they are positioned at the beginning of the retina; while the photoreceptors (the rods and cones) are the outer part of the retina against the pigment epithelium and choroid. The central part of the retina has a high density of cones while the peripheral part is rod dominated (Purves, 2001). The cones are responsible for color vision at higher light levels while the rods work in low levels of light environments, thus being primarily responsible for night vision. To activate the rods and cones light must travel through the entire thickness of the retina (Fig. 3). When photons are absorbed by the visual pigment of the

photoreceptors, a biochemical message is generated and it is then transformed into an electrical message that travels through the retina and eventually reaches the brain via the optic nerve.

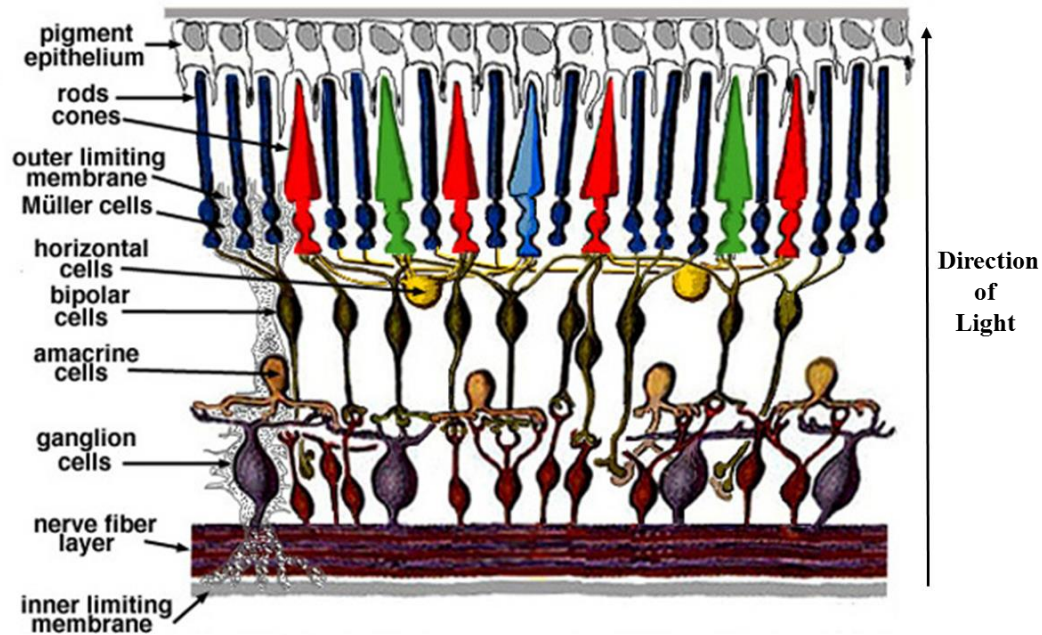


Figure 3: Simple organization of the retina (webvision, 2012).

The strongest refractive surface in the eye is the anterior surface of the cornea; this air-to-cornea interface accounts for about two-thirds of the overall dioptric (i.e. focalization) power of the eye. The remaining refraction mostly occurs on the surface and within the internal stria of the crystalline lens, that normally (long distance sight) contributes by 1/3 to the total dioptric power but can augment its focalization when focusing on a close object.

The refractory index n of a medium reflects the percentage amount by which the traveling light is slowed down. As an approximation, in air $n = 1$, i.e. light travels at approximately the same velocity as in empty space $c = 3000000$ km/sec. In a denser medium like the cornea tissue, $n = 1.38$, and light

will travel at a lower velocity of $v = c/n$. The refraction index difference at the interface between two media causes the refraction phenomenon; i.e. a direction change described by Snell's law (Eq. 1 and Fig. 4):

1.1

$$\frac{\sin \theta_1}{\sin \theta_2} = \frac{v_1}{v_2} = \frac{n_2}{n_1}$$

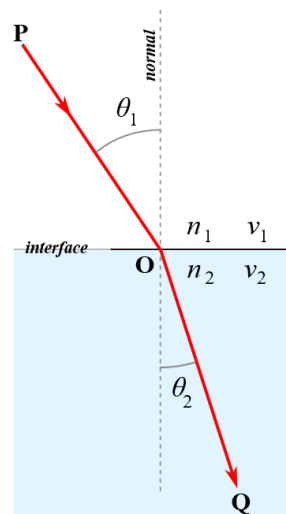


Figure 4: Representation of the Snell's Law.

This phenomenon, with the curvature of a lens surface causes focalization. The dioptric power (DP) grows as the focal point distance f [m] gets narrower and is given by $1/f$ [m^{-1}]. The diopter unit is also indicated as *Diopter Sphere* (DS), originally derived by considering the DP of a spherical lens.

From experimental physiology, it is well known that the human eye resolution is about 1' of arc, i.e. referring to a sinusoid, the eye can discriminate 1 cycle per minute of degree ($1^\circ/60$). Starting from this experimental assumption, it is easy to estimate the maximum spatial resolution on the retina.

Considering the magnification factor, it is possible to demonstrate that 1' of arc corresponds to $5 \mu m$ at the retina.

As regarding the optical properties of the photoreceptors, an important factor to be considered in this work is the numerical aperture (NA). In optics, the NA is a dimensionless number that represents the range of angles to accept or emit light. From the numerical aperture, it can be derived the acceptance angle of an optical system. It has been found that rods acceptance angle is $10^{\circ}2'$, while cones acceptance angle is 26° (Enoch, 1963). The rods and cones are oriented so that the long axis of the outer segment points to the principal point in the eye (within the lens).

1.2 Problem statement

Knowledge of local, effective retinal illuminance is critical to fully interpret results of several tests of retinal function, especially multi-electrode electroretinography, which is the main research focus of the Neural Engineering Vision Laboratory (NEVL) at UIC. The aim of this work is to build a sensor that can allow measurements of absolute retinal illuminance in front of a Ganzfeld source of light and that will be later used to test the effectiveness of the light source at providing uniform retinal illuminance.

1.3 Previous measurements of relative retinal illuminance

Vision research is permeated with studies about theoretical models of human eyes and other species (e.g. Wyszecki & Stiles, 1982; Remtulla and Hallet, 1985; Hughes, 1979), but retinal illuminance has not been investigated deeply yet. This section will analyze the most important papers in this field to understand the scenario in which this thesis takes place.

The most known study on retinal illuminance is probably by Kooijman & Witmer (1986), who measured the retinal illuminance in 3 human and 14 rabbit eyes. They used a small, ball-shaped detector that was introduced at various angles to the optical axis through the back of the excised eye and illuminated from the front with a small Ganzfeld source. All measurements were reported in relative terms because the detector used had isotropic directional sensitivity, and therefore could not be calibrated in any conventional units. Thus, what they obtained were relative amounts of light incident on the given detector location, and no distinction was made between photons arriving along the principle rays entering the eye or photons that were scattered within the eye. This is not a real indicator of effective retinal illuminance from the perspective of a photoreceptor, which has a restricted acceptance angle and a very specific axial alignment, as reported above.

Another study was conducted in 1995 by Williams and Webbers who developed a photometer that measured light transmitted through the sclera of an excised eye (an ocular transmission photometer). This study also reported only relative measurements of retinal illuminance, because the sensor they used had an angular sensitivity that cannot be related to any standard unit of illuminance.

1.4 Light measurement terminology

Here are summarized the terminology and units used in this work related to measurements of light.

Photometric measurements refer to measurements in which the spectral sensitivity of the detector mimics the sensitivity of human photoreceptors. Specifically, it is said to be *scotopic* measurement if it is in the spectral sensitivity of rods; *photopic* in the sensitivity of cones. These spectral sensitivities are based on the CIE standard observer curves (Wyszecki and Stiles, 1982).

Luminance, L , refers to the light flux leaving a distributed source (such as light reflected from a projector screen) per unit area per unit solid angle. Luminance is measured in lumens per meter squared per steradian ($\text{lm m}^{-2} \text{sr}^{-1}$). One lumen per steradian (lm sr^{-1}) is equivalent to one candela (cd).

Illuminance, E , refers to the photometric flux incident on a surface, and is measured in lumens per meter squared (lm m^{-2}).

A *Ganzfeld* source is one that subtends the entire viewing angle of the detector (i.e. the eye in vision research), and has uniform luminance over its entire surface. In practice, a Ganzfeld source is often constructed using an integrating sphere – a hollow sphere the inside of which is painted with a high-diffuse-reflectance coating, and which has ports for viewing and light introduction.

CHAPTER 2

SPECIFIC AIM 1: FABRICATE AN OPTICAL SENSOR SYSTEM THAT MEASURES LOCAL EFFECTIVE ILLUMINANCE IN ABSOLUTE UNITS

2.1 Specific Aim 1 Methods

2.1.1 Construction of Cone-view Sensor

To meet the challenges and overcome the limits of the previous studies mentioned in the first chapter, we have designed a new sensor that approximates the optical properties of a cone photoreceptor cell. To reproduce even better the cone behavior, measurements were taken to test the sensor while it was positioned with its axis pointing toward the exit pupil of a sheep eye, which we will analyze in next chapter. This detector is a “cone-view” sensor, because it approximates the optical properties of a cone cell. To realize the sensor, we did an accurate research of the desired characteristics to reproduce optical properties similar to cone photoreceptors and we then find the right compromises with what was available on the market. The final choice was a Polyimide coated optic fiber with $NA = 0.22$ that works in the visible light wavelengths (390 to 700 nm) (Edmund Scientific, Barrington, NJ). The fiber has an acceptance angle of 25.4° , which is close to angular acceptance of a cone cell (26°). The core diameter is 1000 μm and the external one is 1300 μm . In Figure 5, it is represented the attenuation spectrum of the optic fiber at specific wavelengths, and it is evident that the fiber transmits the visible light. The fiber was cut to a convenient length (about 40 cm). For technical purposes, to transmit light to a photometer, we cut the coating of the fiber at each end for about 2-mm. Each end was then polished using a sequence of 4 sanding sheets with different grits from 1000 to 2500 to remove surface roughness that would effect the angular sensitivity of the device (McMaster-Carr, IL). Each fiber was then analyzed at the surgical microscope to check the results of the polishing procedure. The fiber was interfaced through one end with the detector of a commercial calibrated photometer (IL 1700,

International Light). It was positioned about 1-mm from the surface of a photopic correction filter, which was between the fiber and the silicon photodiode. The other end of the fiber was inserted into a syringe (5 ml) to be easy to handle and fix during the surgical procedure (see Chapter 3).

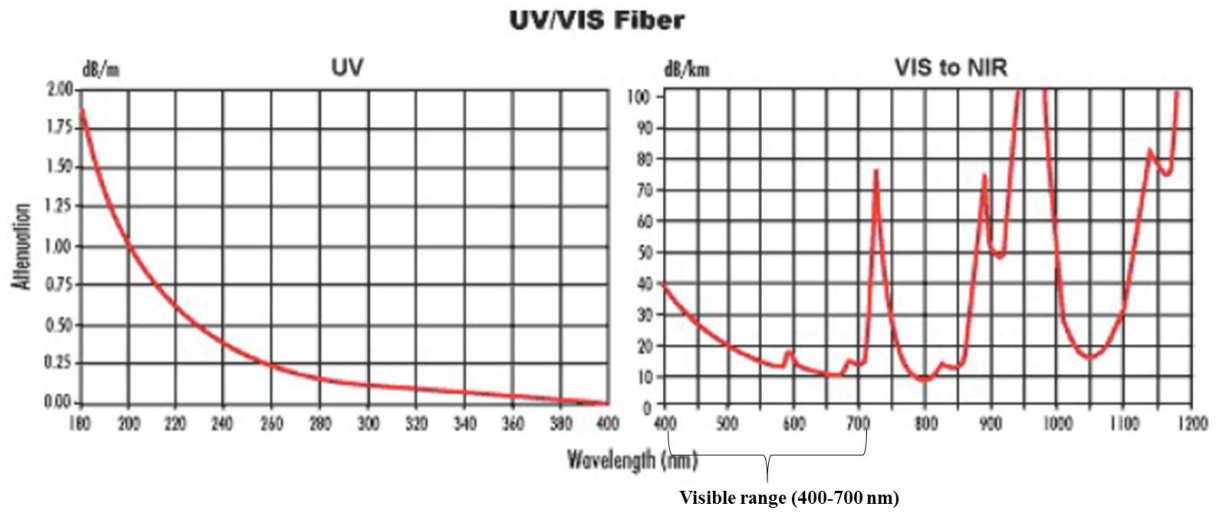


Figure 5: UV/VIS light attenuation at specific wavelength (Edmund Scientific).

2.1.2 Stimulus Source

The source used was the XLamp MC-E LED (Fig. 6), a multi-chip LED that provides high lumen output (Cree, NC). It can reproduce different colour lights, but we used the white one obtained with a power supply set at voltage of 2.5 V and inducing current of 200 mA. The lamp was positioned behind two diffusing screens (Fig. 7). In particular, the aim was to build a source of light that was uniform, so that no differences could be caused by the lamp itself when taking measurements at different orientation angles of the “cone-view” sensor. This is the reason why we used two diffusing screens. To test the effective uniformity of light, we positioned a camera in front of the screens, in total dark conditions of the room, and then used the software *ImageJ* to collect the data from the pictures. We found out that, positioning the diffusing screens at a distance of about 3 inches (7.62 cm), the illuminance was quite uniform all over the picture taken, with an average result of 199,99 scotopic candela per meter squared (sc cd m^{-2}) and a standard deviation of 2.71.

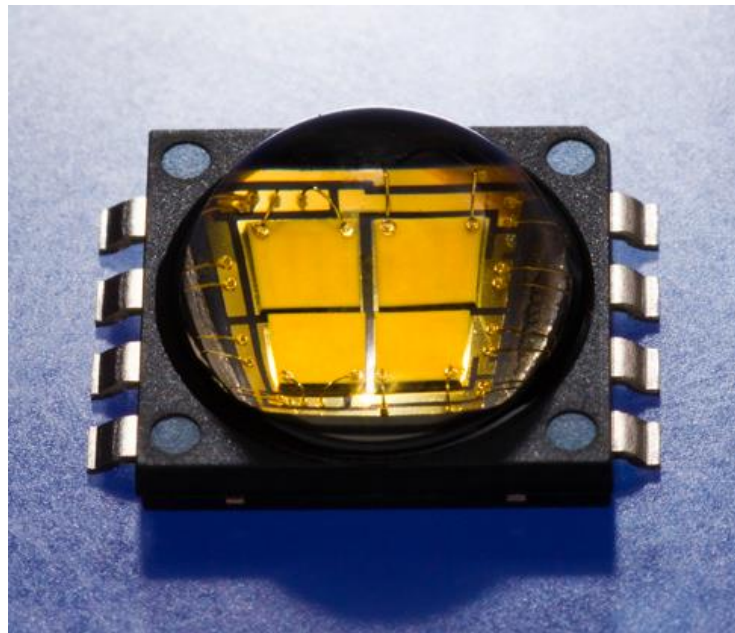


Figure 6: Cree XLamp MC-E LED (Cree Data Sheet).

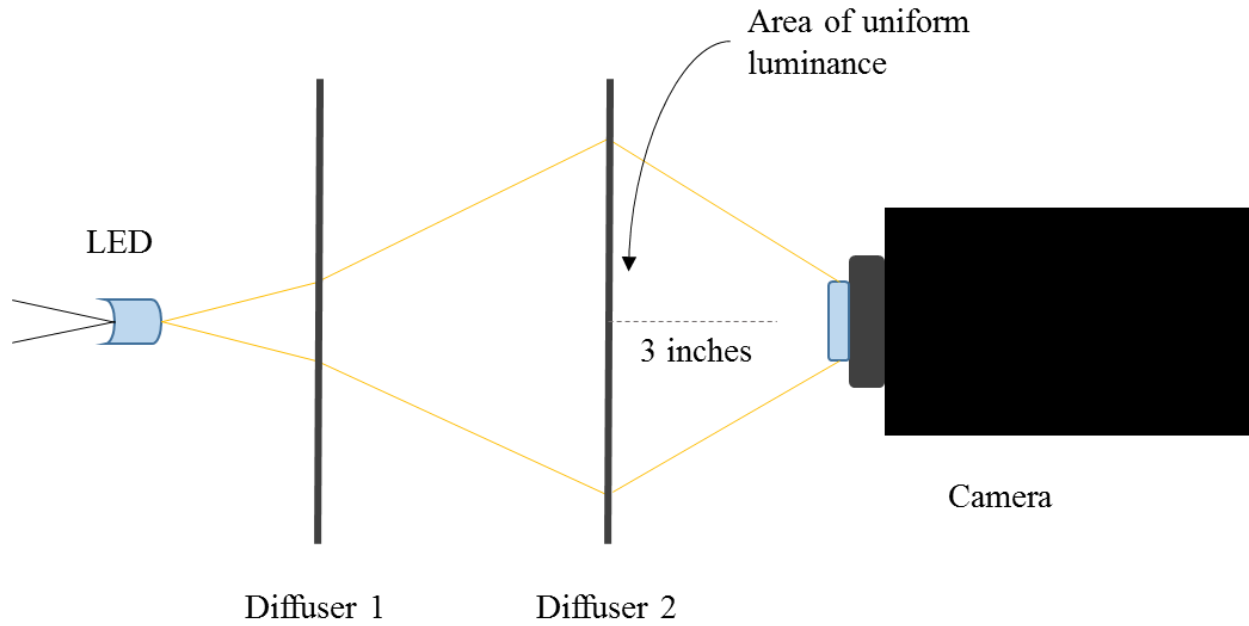


Figure 7: Scheme of the stimulus source positioning.

2.2 Specific Aim 1 Results

Figures 8 and 9 show the results of the “Cone-view” sensor that was built.

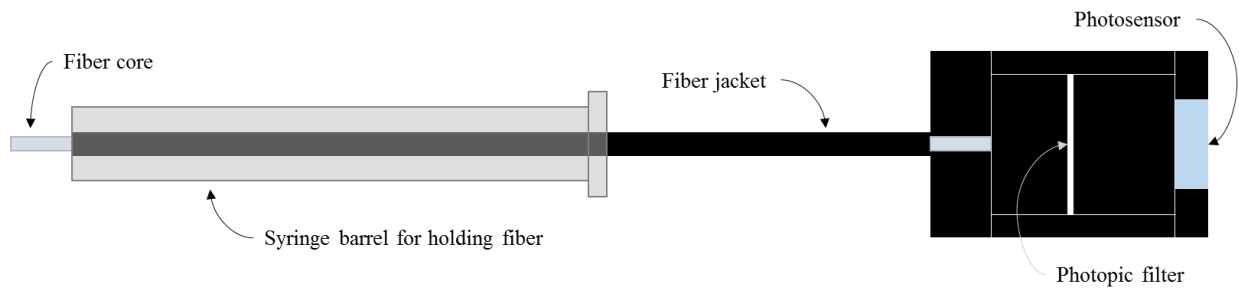


Figure 8: A schematic picture of the system realized with the main components: fiber core, fiber cladding, syringe; photopic filter and photosensor.

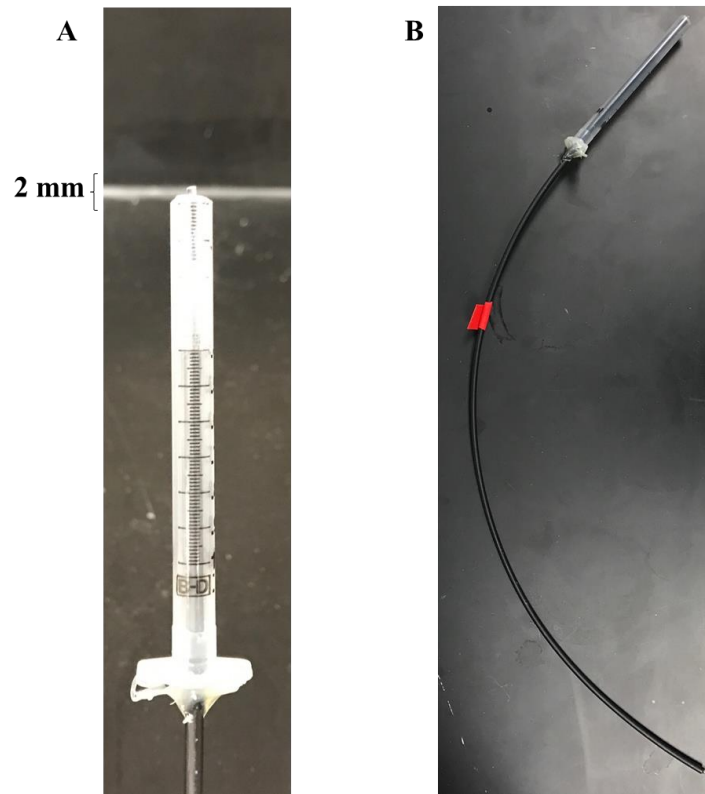


Figure 9: Cone view sensor. A. Frontal view of one end. It gets 2 mm outside the syringe. B. Up view.

2.2.1 Calibration of the cone-view sensor

The calibration was performed on a commercial calibrated illuminance detector (with a cosine response), placed in front of the stimulus source with a fixed setting on the lamp power supply. The illuminance obtained was in $cd\ m^{-2}$. The same setting was used to perform the same stimulus strength for our sensor interfaced with the photometer as described above. The sensitivity factor applied to the recorded photocurrent was adjusted until the photometer reading was the same as it was with the calibrated cosine-response detector. The photometer now read in “effective $sc\ cd\ s\ m^{-2}$ ”.

CHAPTER 3

SPECIFIC AIM 2: MEASURE THE RETINAL ILLUMINANCE IN SHEEP EYES

3.1 Specific Aim 2 Methods

3.1.1 Design of the eye holder and sensor positioning system

To take measurements of retinal illuminance we designed a system to hold the eye and allow inserting the sensor at specific angles from the central axis of the eye. The system was constituted by different pieces assembled together, a ruler and a series of mechanisms to adjust the position of the “cone-view” sensor. The eye holder built is shown in the following pictures (Fig. 10 – 11 – 12).

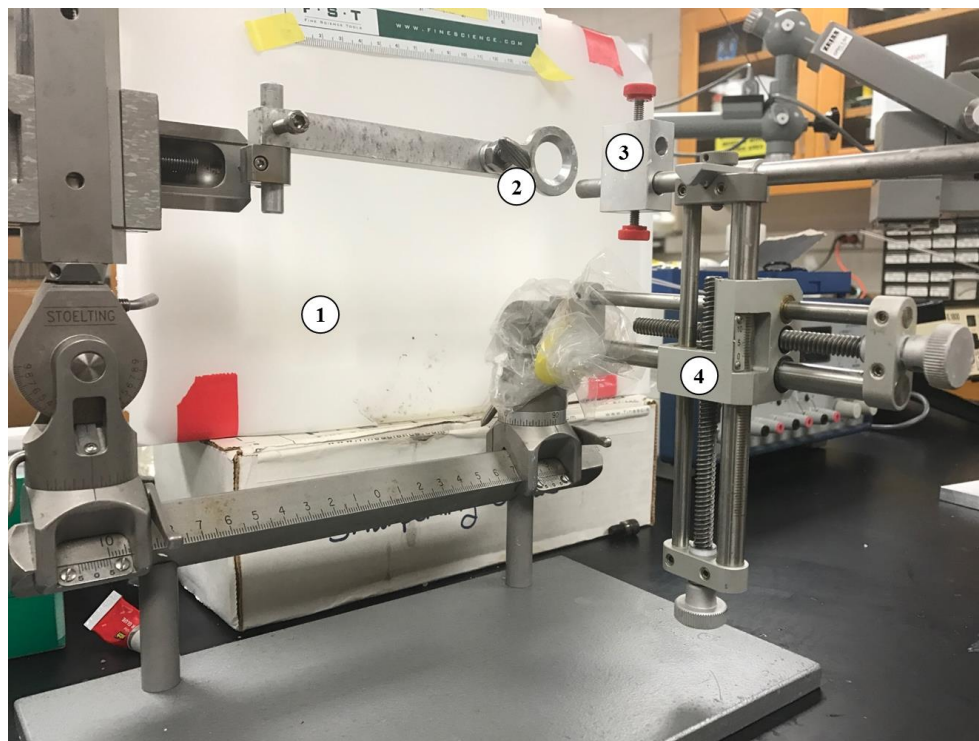


Figure 10: Eye holder and positioning system. Lateral view. 1. Lamp; 2. Eye holder ring; 3. Sensor holder; 4. Components for angular alignment.

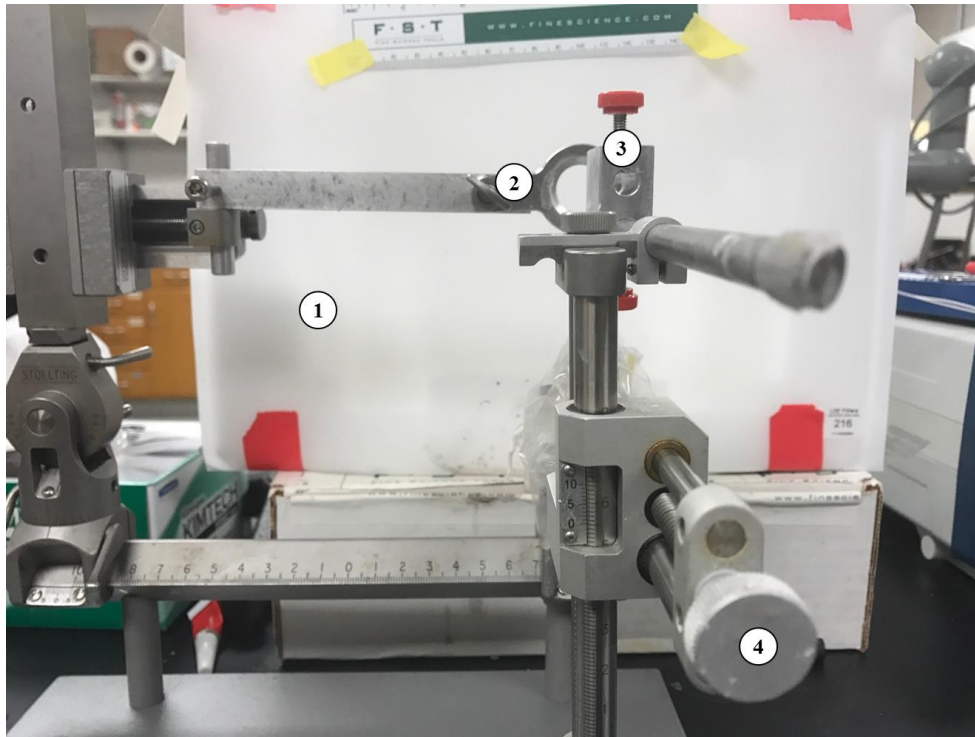


Figure 11: Eye holder and positioning system. Frontal view. 1. Lamp; 2. Eye holder ring; 3. Sensor holder; 4. Components for angular alignment.

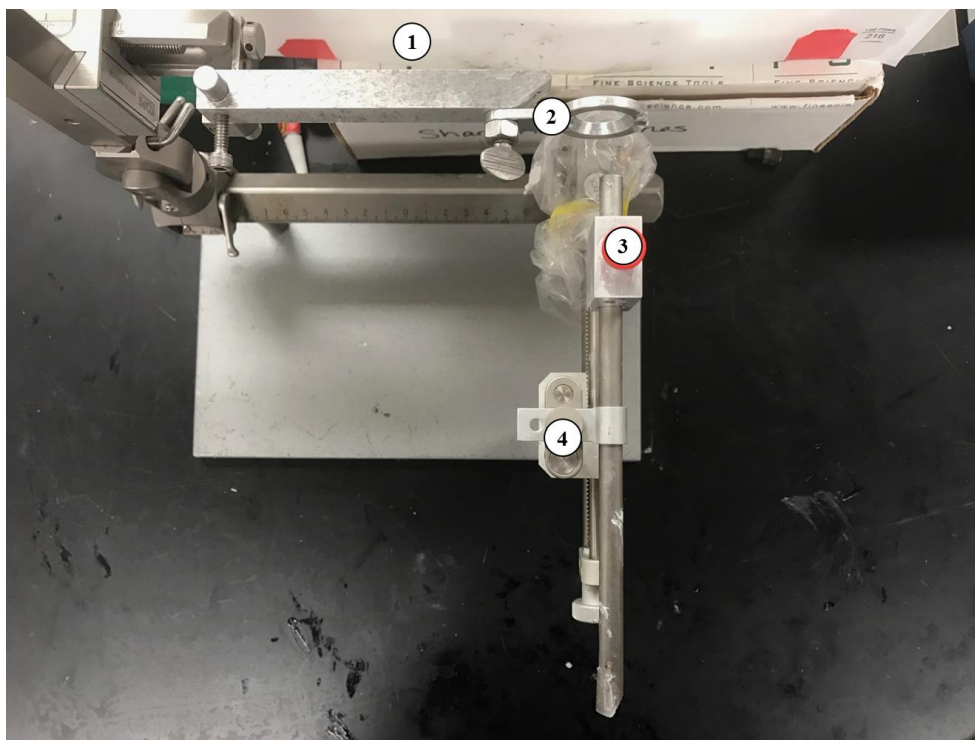


Figure 12: Eye holder and positioning system. Up view. 1. Lamp; 2. Eye holder ring; 3. Sensor holder; 4. Components for angular alignment.

3.1.2 Measurement Protocol

Measurements of retinal illuminance to test the sensor were made on 6 sheep eyes taken from a slaughterhouse in Chicago. To preserve the anatomy and the optical properties of the eyes, they were put into a saline solution and all the experiments were taken within one hour since they had been excised. Each eye was positioned on the eye holder and fixed to it through super glue (Fig. 11). All experiments were taken in dark conditions of the room, with the setting of the lamp as mentioned in the previous chapter. Measurements of retinal illuminance were made in 3 positions for each eye, at 0, 30 and 45 degrees. The detector was positioned to face the exit pupil, for axial alignment similar to photoreceptors. Luminance measurements are reported in $lm\ sr\ m^{-2}$. Figures 13 to 16 show the positioning system and the eyes and sensors used during experiments.

In order to insert the sensor into the eyes, we developed a surgical procedure under the surgical microscope and to evaluate differences in the measurements caused by the surgical approach, we did several trials. The procedure starts with elimination of all tissues and muscles that surrounds the eye. Then proceeds creating a whole through a surgical scalpel in the corresponding point of the eye in which the sensor has to be inserted. Not to create a whole through the entire retina, it is important not to overcome all the tissues and to stop the incision exactly when the retinal pigment epithelium (it appears black) is exposed. The procedure was repeated for all the three angles of the measurements (0, 30, 45 degrees). Saline solution was used to maintain the eye pressure, injected through a syringe.

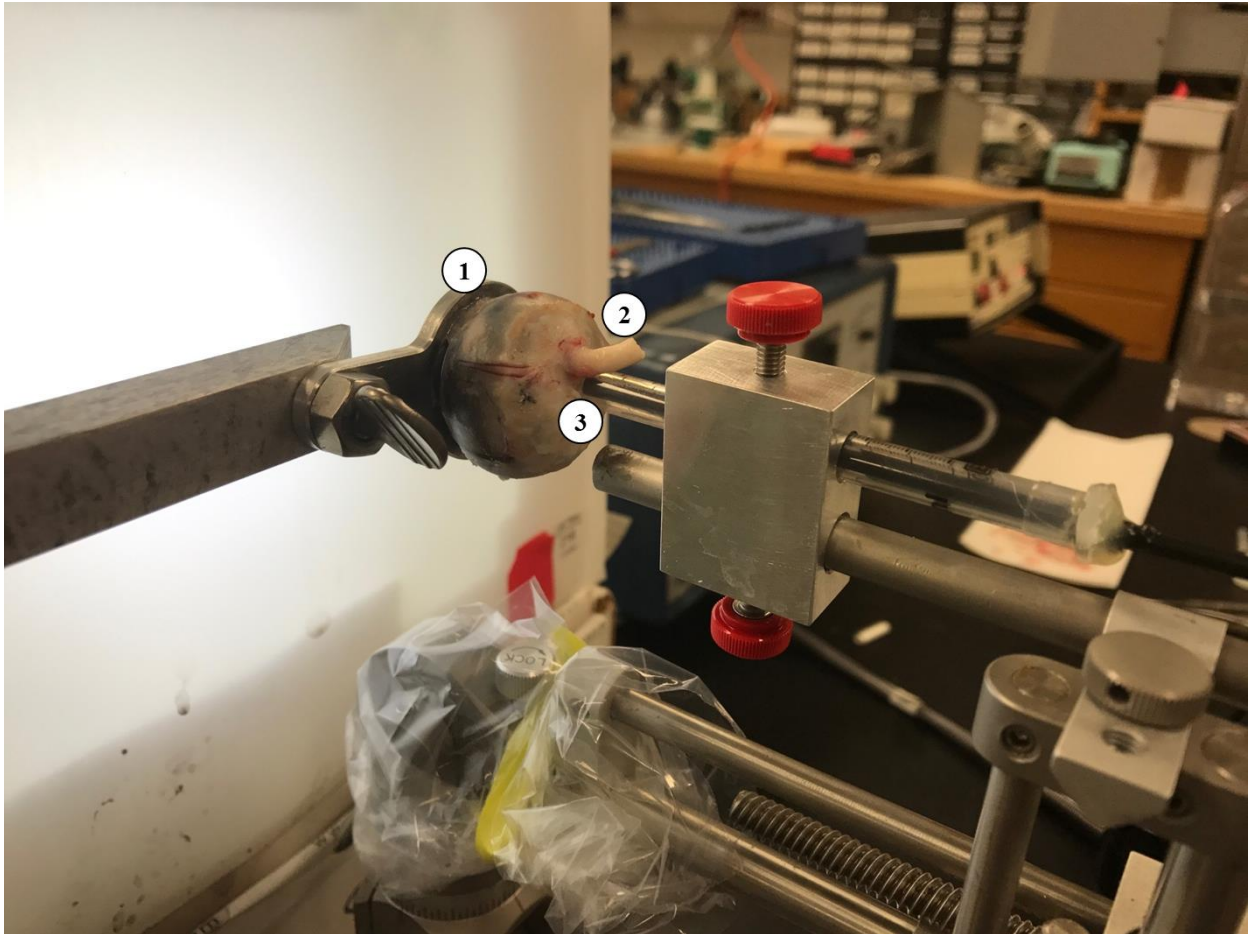


Figure 13: Picture of the measurement system during an experiment. 1. Eye fixed with super glue; 2. Optic nerve; 3. Sensor inserted into the eye at 0° .

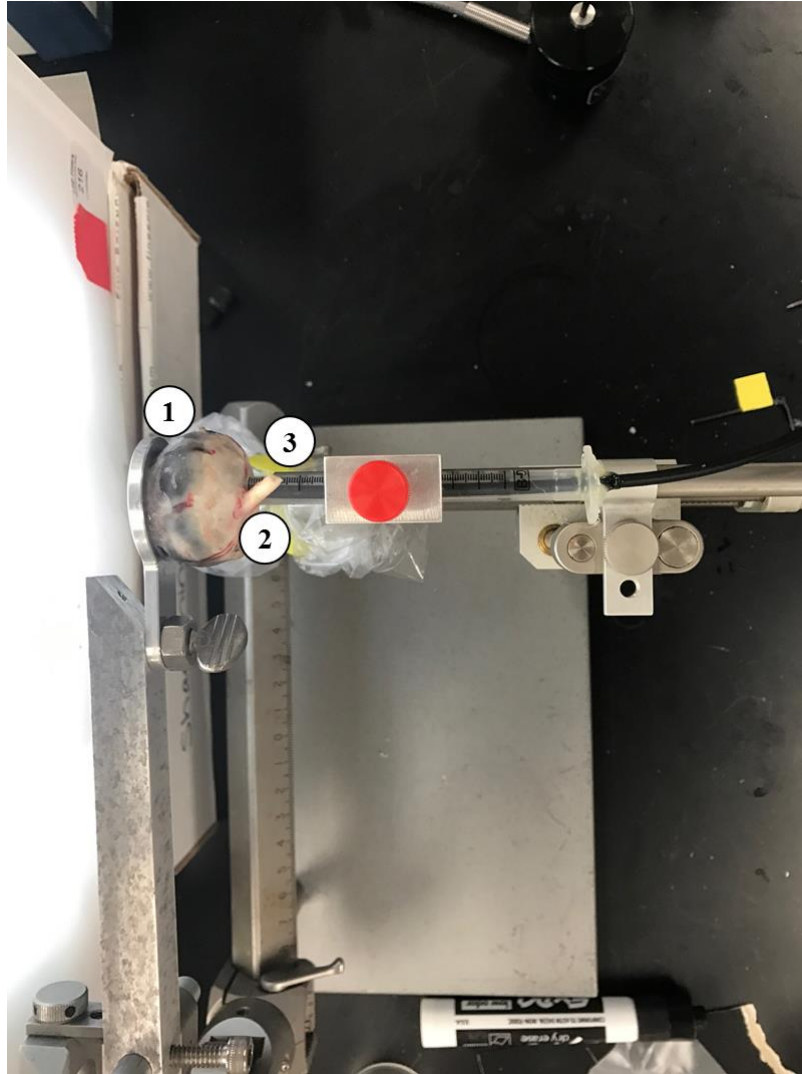


Figure 14: Up view of the measurement system during an experiment. 1. Eye fixed with super glue; 2. Optic nerve; 3. Sensor inserted into the eye at 0° .

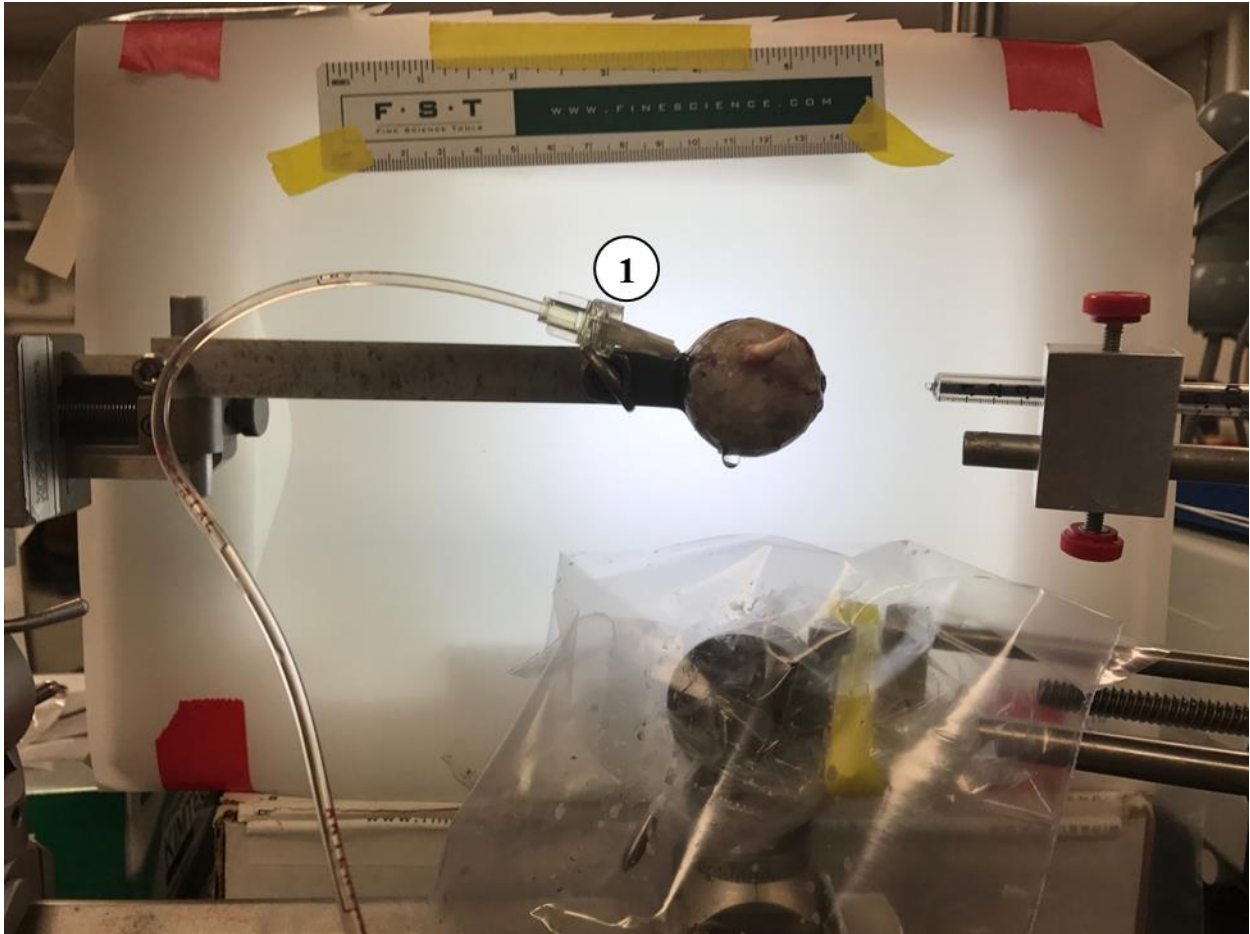


Figure 15: Saline solution used to maintain pressure inside the eye.

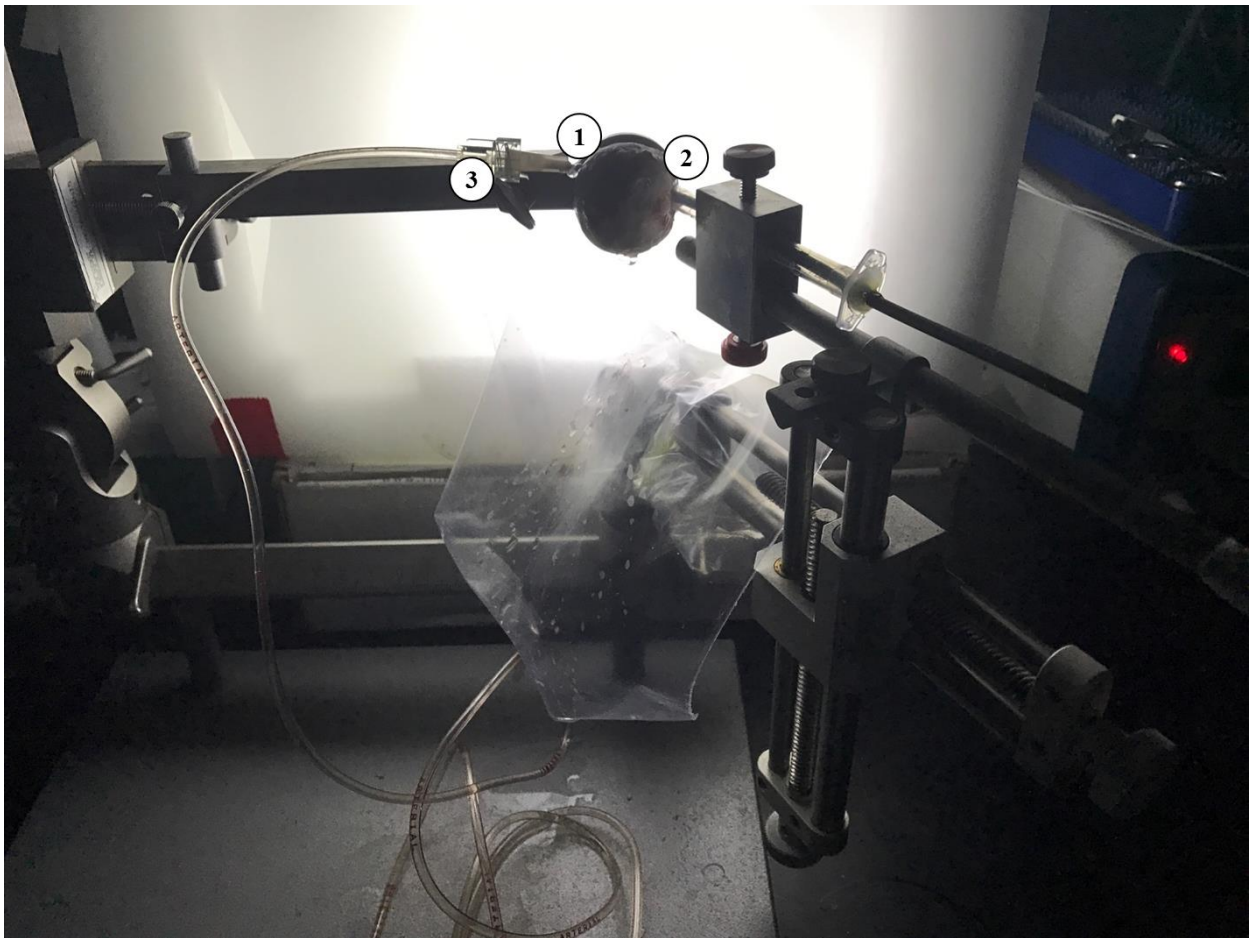


Figure 16: Picture of an experiment in dark condition with the "cone-view" sensor at 45 degrees. 1. Eye; 2. Sensor at 45°; 3. Saline solution syringe.

3.1.3 Analysis Protocol

In order to compensate for differences in eye dimensions, a correction factor was calculated to normalize the data for inter-eye comparison (see the Appendix for the Matlab code used). The principle is that the amount of light entering the eye is proportional to the area of the pupil, and the photon density at the retina is proportional to the area of the retina. The areas of the pupil (A_p) and retina (A_r) were calculated from the measured ocular dimensions (eye diameter; pupil diameter) before each experiment through the use of a ruler. Pupil area was calculated as a circle area with the pupil diameter (πr^2); retina area was approximated to half of a sphere area with the diameter of the entire eye ($2\pi r^2$). The ratio of the two areas was then calculated for each eye (A_p/A_r). Within a set of measurements made under similar conditions, these ratios were normalized to provide a correction factor. Sensor readings of retinal illuminance were then multiplied by this correction factor to provide the numbers reported in the results. The table below shows the eye dimensions used to calculate the correction factors.

Eye Number	Eye diameter		Pupil size	
	inches	mm	inches	mm
EYE 1	1.700"	43.2mm	0.565"	14.35mm
EYE 2	1.195"	30.4mm	0.450"	11.43mm
EYE 3	1.850"	47.0mm	0.516"	13.11mm
EYE 4	1.650"	42.0mm	0.529"	13.44mm
EYE 5	1.103"	28.0mm	0.449"	11.41mm
EYE 6	1.230"	31.2mm	0.695"	17.65mm

Table 1: DIMENSIONS OF THE 6 EYES TO CALCULATE THE CORRECTION FACTORS

Some other steps were performed to analyze the data and see if they were consistent or not. A post-hoc power analysis was performed to check if the measurements obtained were enough to test the hypothesis that there is a difference in retinal illuminance between 0 degrees and 45 degrees.

A repeated-measures ANOVA statistical test was performed on the measurements obtained at 0, 30 and 45 degrees to determine if the different values of retinal illuminance were significant.

At the end, data were compared with the values of retinal illuminance in 3 human eyes found in literature by Kojjiman and Witmer (1986). To perform the comparison, the values obtained by each eye were first normalized to have a value of 1.0 at 0 degrees, then the values across the eyes were averaged and plotted together with Koyjiman and Witmer results. In addition, normalized standard deviations were plotted at each angle.

3.2 Specific Aim 2 Results

The tables below show the measurements of retinal illuminance obtained from 6 sheep eyes for 0, 30 and 45 degrees with respect to the optic axis of the eye. The measure unit is lm sr m^{-2} .

Eye Number	Retinal Illuminance		
	0 degree	30 degrees	45 degrees
EYE 1	$7.96 \cdot 10^{-7}$	$7.49 \cdot 10^{-7}$	$7.13 \cdot 10^{-7}$
EYE 2	$1.56 \cdot 10^{-6}$	$1.31 \cdot 10^{-6}$	$1.11 \cdot 10^{-6}$
EYE 3	$1.45 \cdot 10^{-6}$	$1.07 \cdot 10^{-6}$	$1.14 \cdot 10^{-6}$
EYE 4	$4.24 \cdot 10^{-6}$	$2.44 \cdot 10^{-6}$	$1.58 \cdot 10^{-6}$
EYE 5	$1.97 \cdot 10^{-6}$	$1.54 \cdot 10^{-6}$	$1.06 \cdot 10^{-6}$
EYE 6	$2.83 \cdot 10^{-5}$	$1.41 \cdot 10^{-6}$	$3.17 \cdot 10^{-7}$
Mean Values	$6.39 \cdot 10^{-6}$	$1.42 \cdot 10^{-6}$	$9.89 \cdot 10^{-7}$
St. Dev.	$1.08 \cdot 10^{-5}$	$5.74 \cdot 10^{-7}$	$4.32 \cdot 10^{-7}$

Table 2: MEASUREMENTS OF RETINAL ILLUMINANCE IN ABSOLUTE VALUES [lm sr m^{-2}]

The boxplot in Fig. 17 represents the values of the retinal illuminance found in the experiments using our “cone-view” sensor for the three different angulations of the sensor axis. Figure 18 shows the results after normalization for pupil and eye size.

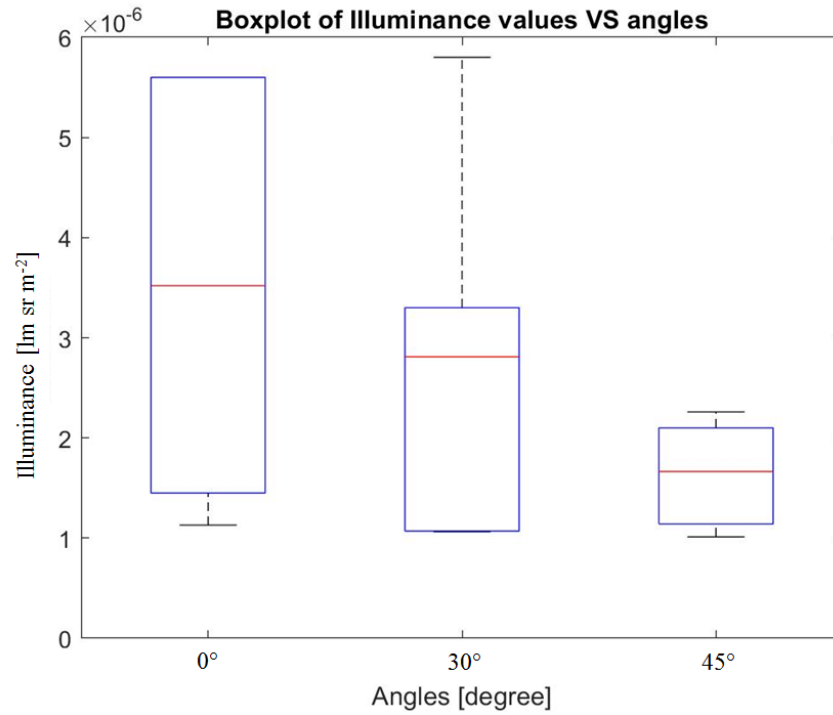


Figure 17: Boxplot of the retinal illuminance before normalization for eye size at 0, 30 and 45 degrees.

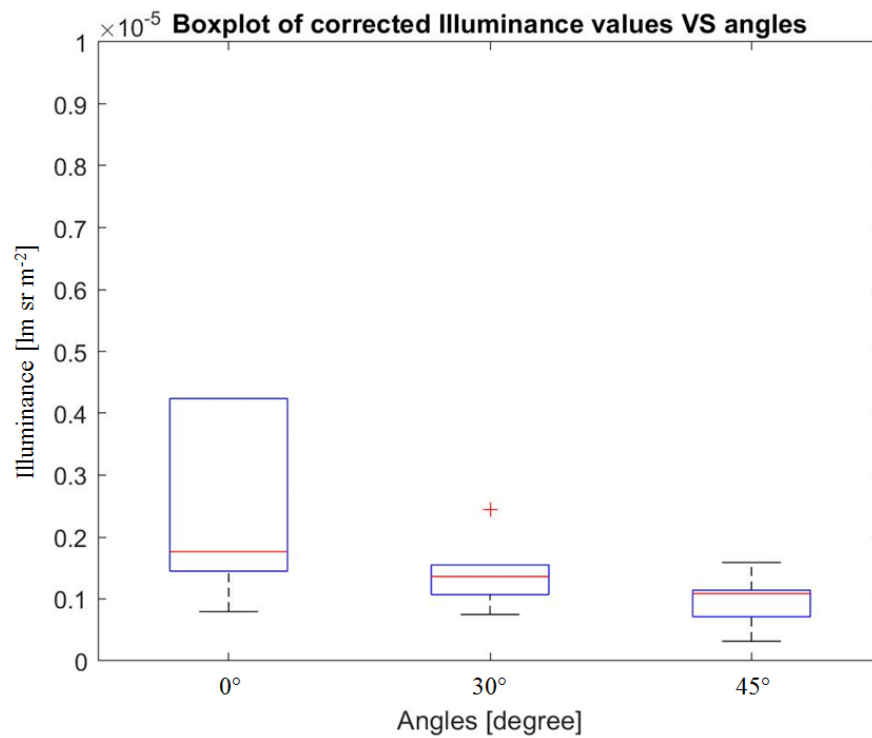


Figure 18: Boxplot of the corrected illuminance values at different angles: 0, 30 and 45 degrees.

One-way ANOVA was performed to evaluate the significance of the different values of illuminance observed at each angle. The resulting p-value was 0.3, well above the criterion value of 0.05. Therefore, the ANOVA suggests that there is no real difference in the values measured at the different angles (i.e. the different retinal positions). However, inspection of Figure 18 suggests that there is a trend of illuminance vs. angular position, with higher illuminance values at the posterior pole of the eye, and lower illuminance values at more peripheral locations. A post-hoc power analysis used to compare the observed effect size at 0 and 45 degrees revealed a power of 23.2%, well below the criterion level of 80% typically considered as sufficient for biomedical studies. Therefore, the number of measurements made in this study ($n = 3$ eyes) was not sufficient to determine with confidence the values at the different retinal positions. A trend of reduced retinal illuminance at more peripheral retinal locations may in fact exist, but more measurements will need to be made to determine this with statistical certainty. Using an online sample size calculator, the means and standard deviations observed in these three eyes (at 0 and 45 degrees) were used to estimate the minimum number of eyes that would be required to achieve confidence in the ANOVA results; a total of 25 eyes will need to be examined in this new system.

Figure 19 shows the results of the comparison with the retinal illuminance values found in literature (Koyjiman and Witmer, 1986). A similar trend of reduced illuminance with eccentricity can be seen in both data sets. The greater reduction in observed retinal illuminance observed in the current study is likely due to the more limited acceptance angle of the sensor used. Recall that the sensor used here had an acceptance angle that mimics the cone photoreceptors, while the sensor used by Koyjiman and Witmer (1986) has a much wider acceptance angle.

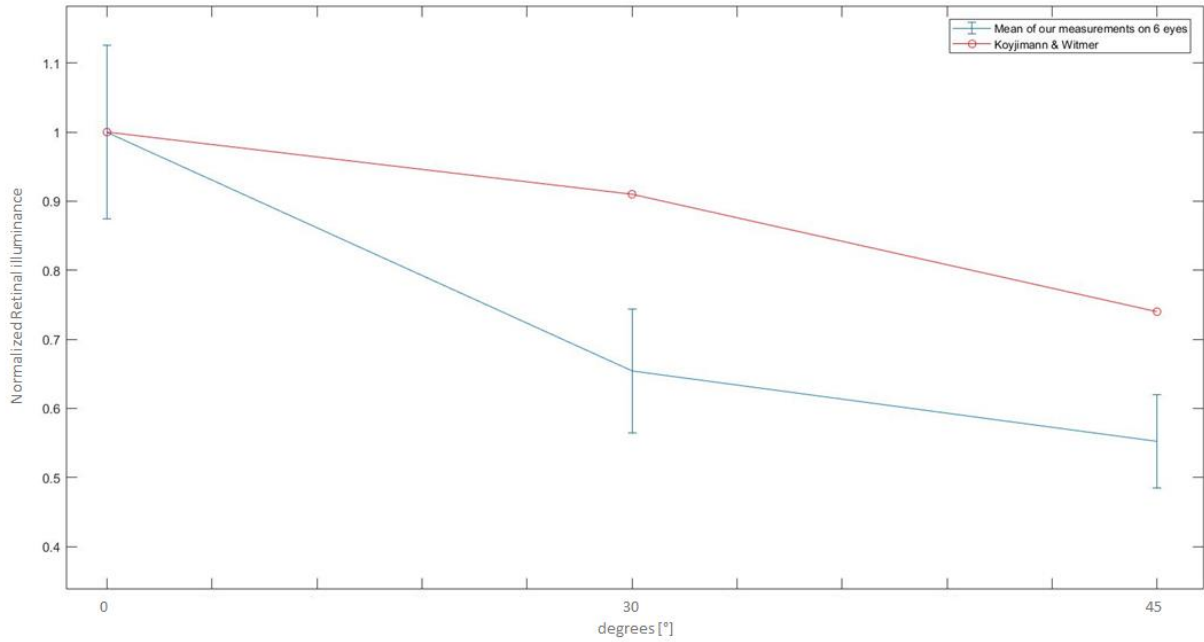


Figure 19: Comparison between our results and those reported by Koyjiman and Witmer (1986). Both data sets were normalized by dividing the mean and standard deviation at each angle by the mean observed at 0 degrees.

CHAPTER 4

DISCUSSION

This thesis has achieved the realization of the first sensor to measure retinal illuminance in absolute units. The sensor approximates the acceptance angle of a cone photoreceptor cell, and if positioned such that its axis is aligned in the anatomically correct orientation for cones at the locus of the measurement within the retina, it allows to measure effective retinal illuminance for cone photoreceptors. The sensor designed is different from all the ones already found in literature because it approximates the optical properties of a cone photoreceptor cell. Till now, measurements obtained in literature have been referred only in relative values and we have provided a good measuring approach to obtain values in absolute units.

A first test of the sensor has been done on sheep eyes that were the only ones available for the strict times and constraints of this work. The results have shown that retinal illuminance decreases from the center (0 degrees) to different angles from it (30 – 45 degrees) more and more. The results have also shown that different eyes have similar measurements between them. The results of the ANOVA suggest no significant difference in measured illuminance at the three positions examined in this study (0, 30, 45 degrees). However, this is unlikely given the basic optics of the eye, and in disagreement with the trend reported in earlier work. The high p-value is most likely due to the wide variance in our measured values across the three eyes. Even after accounting for the different eye sizes (Figure 18), the variance was still quite high. These differences might be due to RPE adhering to the sensor tip during insertion, to differences in opacity of the ocular media (cornea and lens), to differences in the positioning of the eye on the eye holder ring, or other sources of experimental variability that were not effectively controlled for. However, the high p-value has little meaning because of the low statistical power of 23.2%. To continue this work, these sources of experimental variability should

be identified and minimized, and more measurements should be made, so that an acceptable level of statistical power can be achieved.

Future developments would include realizing a better measuring system creating a high-tech Ganzfeld light source (we would suggest an hemisphere made by LEDs). Next steps would include to test the sensor on human eyes to obtain, for the first time in literature, retinal illuminance measurements in absolute units. These results would be useful for ophthalmology and bioengineering of the eye to design prostheses that could take into account real illuminance. The sensor built will be extremely useful also for electroretinography studies, e.g. it will allow to test the uniformity of the Ganzfeld source of light (necessary condition for this technique).


```
boxplot([vect0, vect30, vect45])
ylim([0,6*10^-6])
xlabel('Angles [degree]')
ylabel('Illuminance')
title('Boxplot of Illuminance values VS angles')
```

```
%% Elaboration of data through the correction factors
```

```
vect0_corrected = vect0.*correctionfactors;
vect30_corrected = vect30.*correctionfactors;
vect45_corrected = vect45.*correctionfactors;
```

```
mean(vect0_corrected)
mean(vect30_corrected)
mean(vect45_corrected)
```

```
figure(2)
boxplot([vect0_corrected, vect30_corrected, vect45_corrected])
ylim([0,1*10^-5])
xlabel('Angles [degree]')
ylabel('Illuminance corrected')
title('Boxplot of corrected Illuminance values VS angles')
```

%% COMPARISON WITH KOYJIMAN AND WITMER

% Vectors of values for each eye and their normalization to the 0 degree value.

```
vocchio1 = [7.96*10^-7;7.49*10^-7;7.13*10^-7];
vocchio1norm = vocchio1./vocchio1(1);
```

```
vocchio2 = [1.56*10^-6;1.31*10^-6;1.11*10^-6];
vocchio2norm = vocchio2./vocchio2(1);
```

```
vocchio3 = [1.45*10^-6;1.07*10^-6;1.14*10^-6];
vocchio3norm = vocchio3./vocchio3(1);
```

```
vocchio4 = [4.24*10^-6;2.44*10^-6;1.58*10^-6];
vocchio4norm = vocchio4./vocchio4(1);
```

```
vocchio5 = [1.97*10^-6;1.54*10^-6;1.06*10^-6];
vocchio5norm = vocchio5./vocchio5(1);
```

```
vocchio6 = [2.83*10^-5;1.41*10^-6;3.17*10^-7];
vocchio6norm = vocchio6./vocchio6(1);
```

% Vectors of normalized values at 0, 30 and 45 degrees.

```
vocchio0 = [vocchio1norm(1); vocchio2norm(1); vocchio3norm(1); vocchio4norm(1);
vocchio5norm(1); vocchio6norm(1)];
```

```
vocchio30 = [vocchio1norm(2); vocchio2norm(2); vocchio3norm(2); vocchio4norm(2);
vocchio5norm(2); vocchio6norm(2)];
```

```
vocchio45 = [vocchio1norm(3); vocchio2norm(3); vocchio3norm(3); vocchio4norm(3);
vocchio5norm(3); vocchio6norm(3)];
```

% Vectors of our results and the koyjiman results.

```
vocchiogiaco = [1; mean(vocchio30); mean(vocchio45)];
vocchiokoy1 = [1; 0.91; 0.74];
```

% Vectors of our normalized standard deviation

```
err = [0.08*10^-5; 5.74*10^-7; 4.32*10^-7];
errnorm = err./(6.39*10^-6);
```

% Plots

```
figure()
errorbar(vocchiogiaco, errnorm)
hold on
plot(vocchiokoy1, 'ro-')
legend('Mean of our measurements on 6 eyes','Koyjimann & Witmer')
xlabel('degrees [°]')
ylabel('Illuminance [lm sr m^-2]')
legend('Mean of our measurements on 6 eyes','Koyjimann & Witmer')
```

REFERENCES

- [1] Encyclopedia Britannica Macropedia, *Sensory Reception*, USA: Britannica Inc, 1997.
- [2] Kolb, H., *The neural organization of the human retina*, In Principles and practises of clinical electrophysiology of vision, St. Louis, p 25-52, 1991.
- [3] Sally Wu, *Optometry Tidbit*, UCLA.
- [4] Polyak, S. L., *The retina*, Chicago: University of Chicago Press, 1941.
- [5] Van Buren, J. M., *The retinal ganglion cell layer*, Springfield, 1963.
- [6] Jonas, J. B. et al., *Human optic nerve fiber count and optic disc size*, Investigative Ophthalmology and Visual Science, 33 (6), 1992.
- [7] Purves, D., Augustine, G.J., Fitzpatrick, D. et al., *Anatomical Distribution of Rods and Cones*, editors. Neuroscience. 2nd edition. Sunderland (MA): Sinauer Associates, 2001.
- [8] Enoch, J. M., *Optical Properties of the Retical Receptors*, Journal of the Optical Society of America, vol. 53, 1, 1963.
- [9] Kooijman, A.C. and Witmer, F. K., *Ganzfeld light distribution on the retina of human rabbit eyes: calculations and in vitro measurements*, Journal of the Optical Society of America 3:2116-2120, 1986.
- [10] Williams, T. P. and Webbers, P. P., *Photometer for measuring intensity and rhodopsin distribution in intact eyes*, Applied Optics 34:5720-5724, 1995.
- [11] Wyszecki, G. and Stiles, W. S., *Color Science: Concepts and Methods. Quantitative Data and Formulae*, John Wiley & Sons, pp. 98-105, 1982.

VITA

NAME: Giacomo D'Alessandro

EDUCATION: Scientific High School Diploma (2007-2012), Liceo Scientifico Dante Alighieri, Matera, Italy

Bachelor of Science in Biomedical Engineering (2012-2015),
Politecnico di Milano, Milan, Italy

Master of Science in Biomedical Engineering (2015-2017), Politecnico di Milano, Milan, Italy

Master of Science in Biomedical Engineering (2015-2107), Politecnico di Torino, Turin, Italy

Alta Scuola Politecnica (2015-2017), Italy

Master of Science in Bioengineering (2016-present), University of Illinois at Chicago, Chicago, USA

WORK EXPERIENCE: Analyst (2017-present) for Deloitte Consutling srl, Health Care & Life Sciences, Milan, Italy